Electronic Supplementary Material (ESI) for Journal of Materials Chemistry C.

Enhancement in the efficiency of $Sb_2(S,Se)_3$ thin-film solar cells with Spin-coating NiO_x as the hole transport layer

Shan Huang[a#], Yelei Xing[b#], Honcheng Zhu[a], Tingyu Zhang[b], Kangjun Geng[a], Yusheng Yang[b], QingYan Gu[a], Sai Jiang[a], Jianhua Qiu[a]*, Huafei Guo[a]*, Ningyi Yuan[b], and Jianning Ding[c]*

[a] *School of Microelectronics and Control Engineering, Changzhou University, Changzhou 213164, China*

[b] *School of materials science and engineering, Changzhou University, Changzhou, 213164, China*

[c] *Yangzhou University Technological Institute of Carbon Neutralization, Yangzhou University, Yangzhou, 225127, China*

The author contributes equally to this work

E-mail: guohuafei@cczu.edu.cn; saijiang@cczu.edu.cn; jhqiu@cczu.edu.cn;

1. Experimental details

1. 1. Device fabrication

First, the FTO substrate was ultrasonically cleaned with detergent, ultrapure water, and ethanol for 30 min and treated with ozone for 15 min. A 60-nm film of CdS was then deposited on the FTO as an electron transfer layer using chemical bath deposition for 6 min. The coating was spun with $CdCl_2$ (20-mg mL^{-1} cadmium chloride methanol solution) for 30 s at 3000 rpm, followed by annealing at 400 ℃ for 10 min and a natural cooling process. $Sb_2(S,Se)_3$ films were deposited on CdS substrates using a hydrothermal method with a modified 0.2671 g of $KSbC_4H_4O_7·0.5H_2O$, 0.7942 g of $Na_2S_2O_3·5H_2O$, 0.02 g of CH_4N_2Se, 0.04 g of EDTA, and 0.25 g of NH_4F were added to a Teflon jar (50 ml) with 40 ml of ultrapure water and heated in a drying oven at 130 ℃ for 180 min to perform a hydrothermal reaction. Next, ultrapure water was used to wash the samples and the resulting $Sb_2(S,Se)_3$ films were placed under a nitrogen atmosphere and annealed at 350℃ for 15 min. Furthermore, NiO_x film were deposited on $Sb_2(S,Se)_3$ using the spin-coating method. The spin-coated NiOx films were then placed on a hot table and annealed under an air atmosphere. Finally, Thermal evaporation was used to create gold electrodes with a surface area of 0.07 cm^2 and a thickness of 60 nm.

1.2. Measurements and characterization

The surface morphologies of the NiO_x and $Sb_2(S,Se)_3$ films were characterised by scanning electron microscopy (SEM, SEM-S4800, Hitachi). The surface roughness of the NiO_x and $Sb_2(S,Se)_3$ films was characterised using atomic force microscopy (AFM; Nano Man VS, Veeco). XRD patterns of the NiO_x films annealed at different temperatures (Nihon Reiji D/Max 2500PC). The elemental composition of NiO_x films was determined using X-ray photoelectron spectrometry (XPS). The current density–voltage (J–V) curves of the $Sb_2(S,Se)_3$ thin-film solar cells were simulated using a source metre (2400) under standard illumination (100 mW cm^{-2}). The dark J–V curves of the devices were measured from −1 to +2 V under dark conditions. A photovoltaic characterisation system (QEXL) was used to determine the solar cells' external quantum efficiency. In complete darkness, electrochemical impedance spectroscopy (EIS) was carried out at 0.60 V from 10 Hz to 4 MHz. Uv-vis spectrophotometry (Shimadzu UV-2600) was used to analyze the optical characteristics of the $Sb_2(S, Se)_3$ and NiO_x films. A PHI 5000 VersaProbe III with a He I source (21.22 eV) and an applied negative bias of 9.0 V was used to conduct ultraviolet photoelectron spectroscopy (UPS). A precision LCR meter (E4980AL) was used to measure capacitive voltage (C-V) in the dark with a bias voltage ranging from -1 to +1 V.

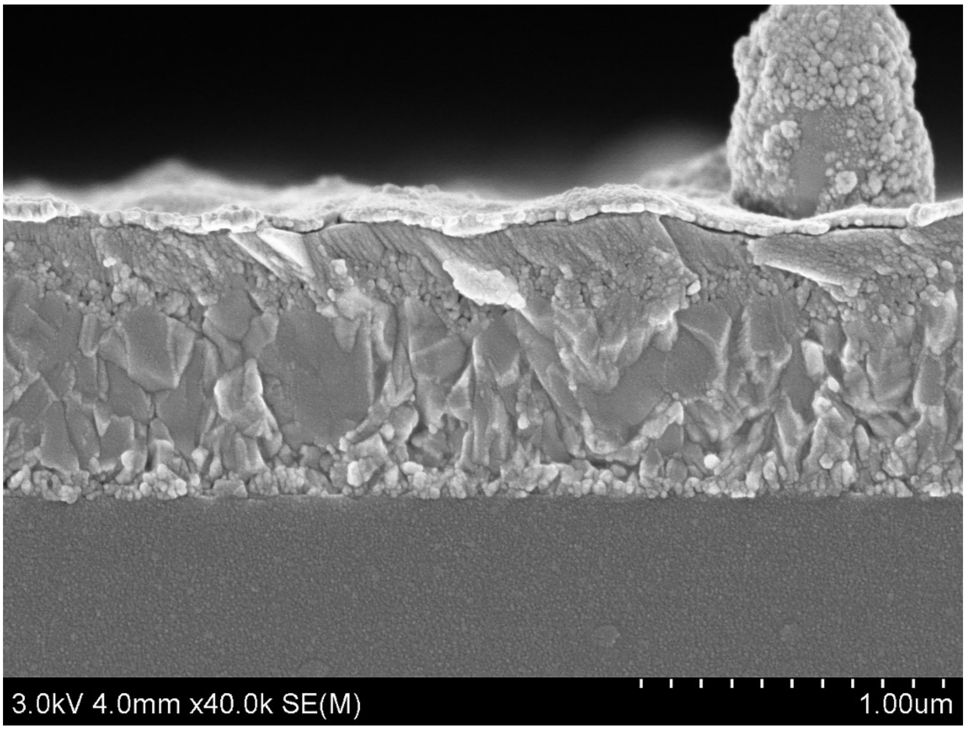

Fig. S1. The cross-sectional SEM image of 2.5 mg mL^{-1}.

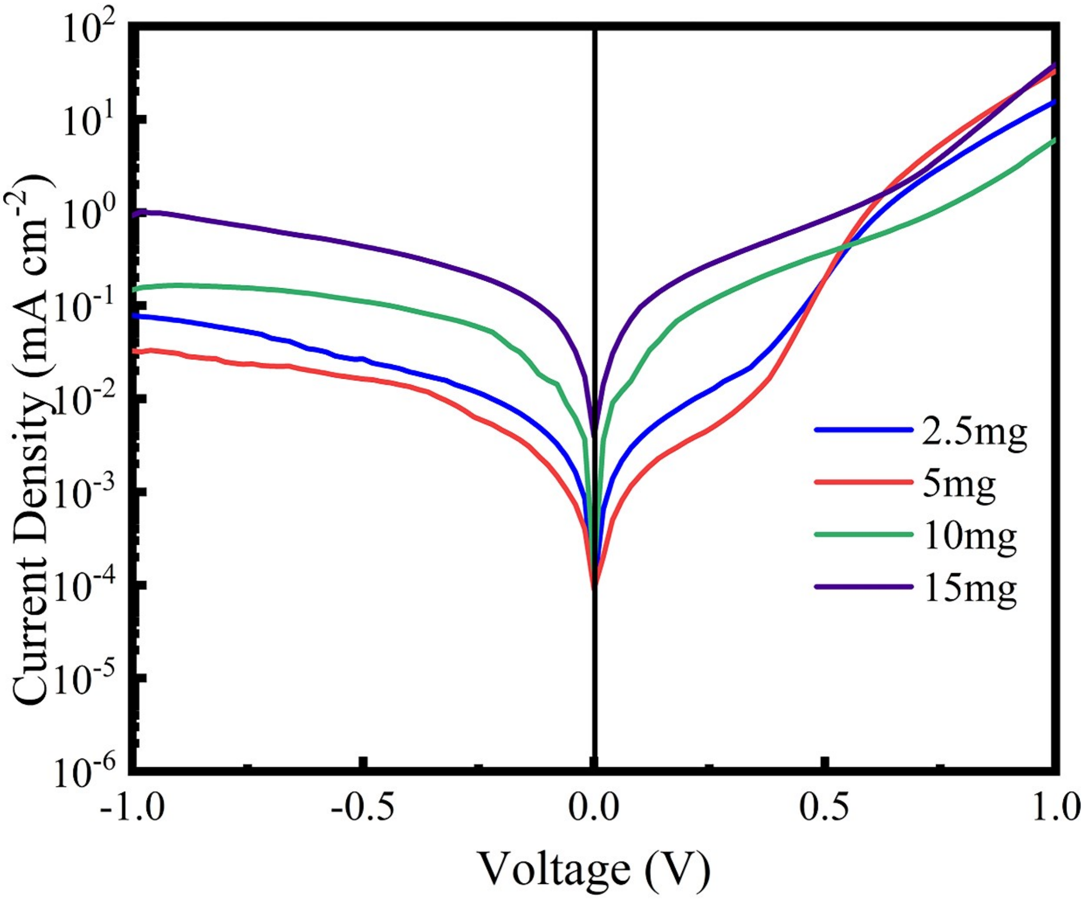

Fig. S2. Dark *J-V* curves of different concentrations

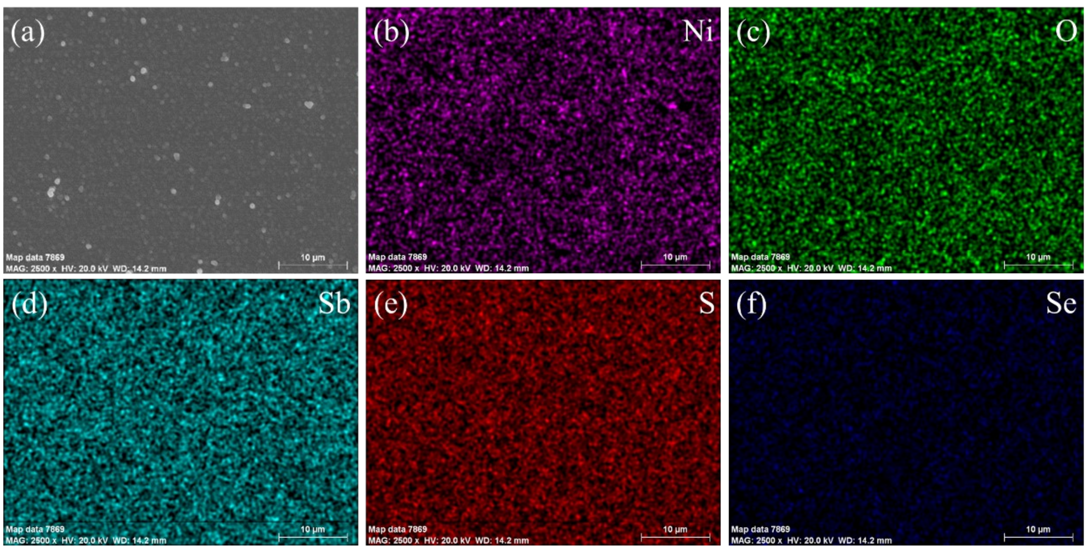

Fig. S3. EDS patterns of $Sb_2(S,Se)_3$ films based on 5 mg mL^{-1} NiO_x.

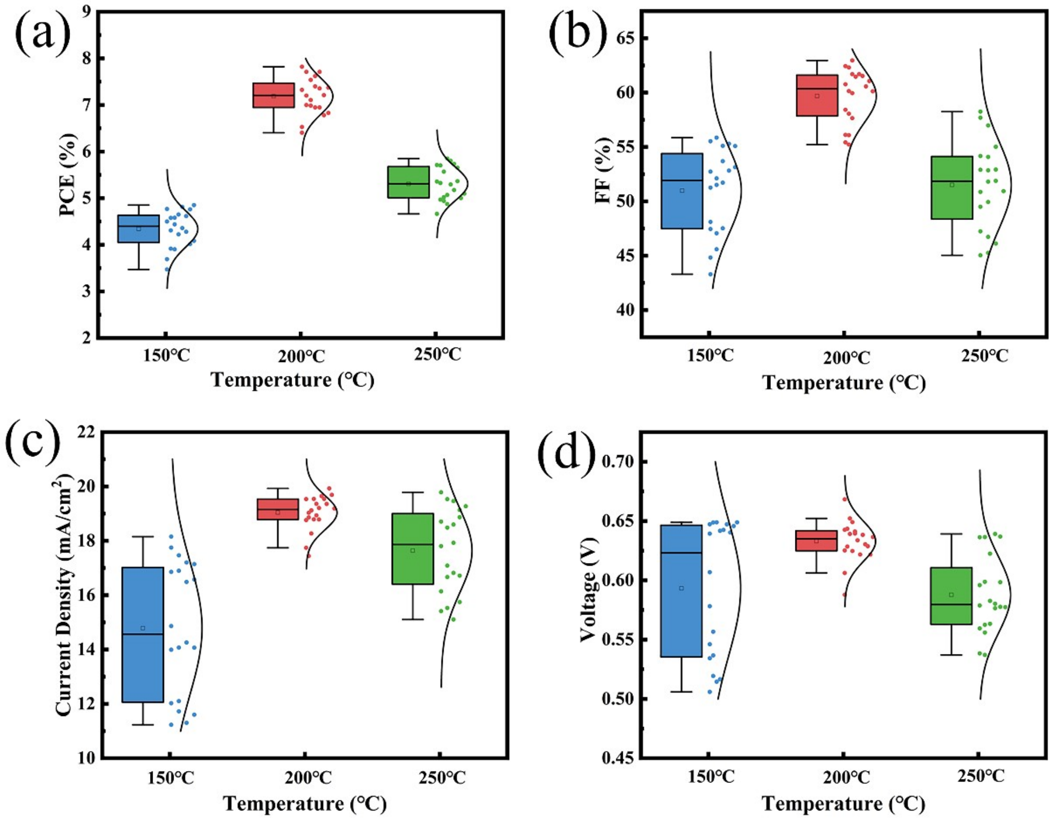

Fig. S4. Photovoltaic parameters based on different temperatures of NiO_x (a) PCE, (b) *FF*, (c) J_{SC}, (d) V_{OC}.

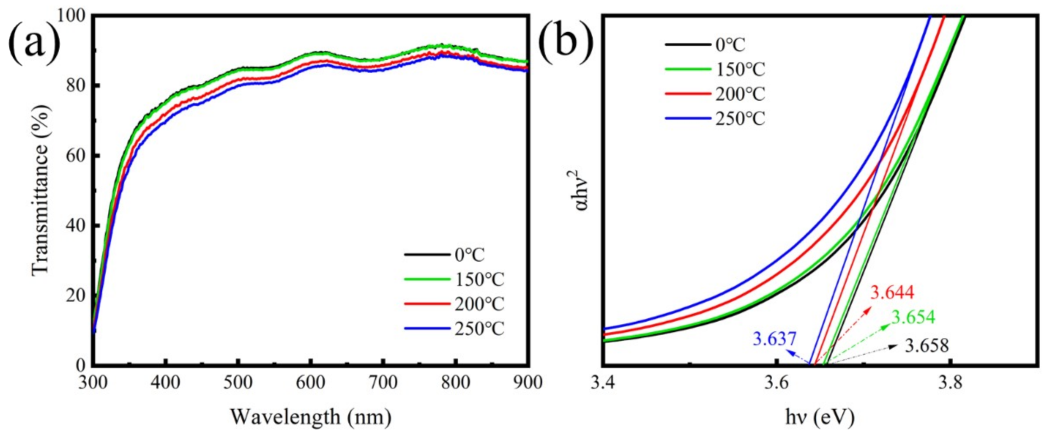

Fig. S5. Solar cells with different annealing temperatures NiO_x as HTL(a) UV-vis transmission spectra, (b) Optical band gap maps.

Table S1 Parameter table of the device with different annealing temperature NiO_x as HTL

Sample	V_{OC} (V)	J_{SC} (mA cm^{-2})	*FF* (%)	PCE (%)	R_S (Ω)	R_{sh} (Ω)
150°C	0.5146	17.14	52.73	4.65	674.5550	22100.60
200°C	0.6214	18.30	57.60	6.55	494.1029	24871.33
250°C	0.6358	16.74	53.43	5.69	414.8466	10420.13

Table S2 Photovoltaic parameters based on 150°C

Sample	**PCE (%)**	***FF* (%)**	**J_{SC} (mA cm^{-2})**	**V_{OC} (V)**
1	3.69171	43.28953	16.85596278	0.505930847
2	4.49999	47.44965	17.75032427	0.534284609
3	4.7698	48.1034	18.1552791	0.546162462
4	4.57642	47.06189	17.46705009	0.556719527
5	5.3347	51.79557	16.9703191	0.606914095
6	3.91836	45.59349	14.86386043	0.578189503
7	4.01617	55.29955	11.30332006	0.642516068
8	4.08616	55.08205	11.60203712	0.63939708
9	4.81232	52.82838	14.0735877	0.647264817
10	4.61608	51.51065	13.99344635	0.640400041

Table S3 Photovoltaic parameters based on 200°C

Sample	**PCE (%)**	***FF* (%)**	**J_{SC} (mA cm^{-2})**	**V_{OC} (V)**
1	7.08442	60.14239	18.33685881	0.642390129
2	7.01097	59.79723	18.38545496	0.637709562
3	7.53757	61.46527	19.20903981	0.638404225
4	7.1064	58.42422	19.03043103	0.639157678
5	7.40649	59.5777	19.42862498	0.639862705
6	7.40	60.1391	19.12125341	0.64351534
7	7.51276	59.45273	19.39016006	0.651697749
8	7.70954	61.06469	19.69195644	0.641135327
9	6.6213	57.04293	18.25138745	0.635983017
10	6.99892	55.42556	19.36140108	0.652205118

Table S4 Photovoltaic parameters based on 250°C

Sample	**PCE (%)**	***FF* (%)**	**J_{SC} (mA cm^{-2})**	**V_{OC} (V)**
1	5.71283	58.24986	15.41303134	0.636310001
2	5.70356	57.69485	15.53072879	0.636527255
3	5.357	56.98004	15.10331821	0.62248128
4	5.32497	52.90714	15.74684271	0.639159886
5	5.56895	54.17266	16.14121255	0.636879125
6	5.02083	45.03661	18.70722872	0.595937072
7	5.85013	52.85174	18.48571287	0.598783361
8	4.66504	45.26224	17.80572554	0.578840919
9	5.07064	54.08005	16.66819935	0.562518553
10	5.29653	55.01408	17.08939128	0.563366408

Table S5 Photovoltaic parameters of devices prepared via different HTLs.

HTL	**PCE (%)**	***FF* (%)**	**J_{sc} (mA cm^{-2})**	**V_{oc} (V)**	**Year**
$CsPbBr_3$[1]	7.82	58.55	21.50	0.62	2020
MnS[2]	9.24	65.48	21.26	0.664	2022
MoO_3[3]	7.20	63	16.53	0.63	2022
CZTS[4]	6.06	54.6	27.12	0.409	2021
CuSCN[5]	7.20	58.1	30.1	0.412	2019
PbS[6]	8.0	65.06	18.8	0.65	2022
NiO_x(Jin)[7]	3.51	40.86	14.50	0.59	2018
NiO_x (this work)	7.40	60.14	19.12	0.6435	2023

[1] C. H. Jiang, J. S. Yao, P. Huang, R. F. Tang, X. M. Wang, X. Y. Lei, H. L. Zeng, S. Chang, H. Z. Zhong, H. B. Yao, C. F. Zhu and T. Chen, Cell Reports Physical Science. 2020, **1** (1), 100001.

[2] S. Y. Wang, Y. Q. Zhao, L. Q. Yao, C. Li, J. B. Gong, G. L. Chen, J. M. Li and X. D. Xiao, Sci Bull (Beijing). 2022, **67** (3), 263-269.

[3] Y. L. Xing, H. F. Guo, J. J. Liu, S. Zhang, J. H. Qiu, N. Y. Yuan and J. N. Ding, Journal of alloys and compounds. 2022, **927**, 166842.

[4] F. L. Mu, Z. Liu, W. Zi, Y. Cao, X.M. Lu, Y. L. Li, Z. Q. Zhao, Z. Y. Xiao and N. Cheng, Solar Energy. 2021, **226**(15), 154-160.

[5] K. H. Li, S. Y. Wang, C. Chen, R. Kondrotas, M. C. Hu, S. C. Lu, C. Wang, W. Chen and J. Tang, Journal of Materials Chemistry A. 2019. **7**(16), 9665-9672.

[6] F. Y. Wu, Y. Q. Zhao, L. Q. Yao, Z. P. Huang, L. M. Lin, Y. P. Ma, S. Y. Chen, J. M. Li and G. L. Chen, Chemical Engineering Journal. 2022, **440**, 135872.

[7] X. Jin, Y. Yuan, C. H. Jiang, H. X. Ju, G. S. Jiang, W. F. Liu, C. F. Zhu and T. Chen, Solar Energy Materials and Solar Cells. 2018, **185**, 542-548.